The EMBO Journal vol.15 no.22 pp.6069–6074, 1996

Myosin motors with artificial lever arms

Michael Anson[1], Michael A.Geeves[2], Susanne E.Kurzawa[2] and Dietmar J.Manstein[1,3,4]

[1]National Institute for Medical Research, Mill Hill, London NW7 1AA, UK, [2]Max-Planck-Institut für Molekulare Physiologie, Postfach 102664, D-44026 Dortmund and [3]Max-Planck-Institut für Medizinische Forschung, Jahnstrasse 29, D-69120 Heidelberg, Germany

[4]Corresponding author

The myosin head consists of a globular catalytic domain and a light chain binding domain (LCBD). The coupling efficiency between ATP hydrolysis and myosin-induced actin movement is known to decline as the LCBD is truncated or destabilized. However, it was not clear whether the observed alteration in the production of force and movement reflects only the mechanical changes to the length of the LCBD or whether these changes also affect the kinetic properties of the catalytic domain. Here we show that replacement of the LCBD with genetically engineered domains of similar rigidity and dimensions produces functional molecular motors with unchanged kinetic properties. The resulting single-chain, single-headed motors were produced in *Dictyostelium discoideum* and obtained after purification from a standard peptone-based growth medium at levels of up to 12 mg/l. Their actin motility properties are similar or greater than those of native myosin. Rates of 2.5 and 3.3 μm/s were observed for motor domains fused to one or two of these domains, respectively. Their kinetic and functional similarity to the extensively studied myosin subfragment 1 (S1) and their accessibility to molecular genetic approaches makes these simple constructs ideal models for the investigation of chemo-mechanical coupling in the myosin motor.

Keywords: actin/α-actinin/*Dictyostelium discoideum*/ molecular motor/spectrin repeat

Introduction

All myosins contain a highly conserved globular catalytic domain that contains the actin and nucleotide binding sites and produces force and movement (Cheney *et al.*, 1993; Goodson and Spudich, 1993). This 'generic' motor domain is attached via a neck region to a variety of functionally specialized tail domains. The neck region consists of an extended, α-helical region that contains binding sites for one or more calmodulin molecules, or calmodulin-like myosin light chains (Figure 1A and B). The neck region of all conventional myosins binds one essential (ELC) and one regulatory light chain (RLC) and is generally referred to as the light chain binding domain (LCBD). In agreement with previous models (Vibert and Cohen, 1988) and based on the atomic structure of the myosin head (Rayment *et al.* 1993a) and of the LCBD alone (Xie *et al.*, 1994; Houdusse and Cohen, 1996), it was suggested that the LCBD acts as a rigid lever arm to amplify small conformational changes in the motor domain, thus producing net movement of filamentous actin of ~5–10 nm per ATP hydrolyzed (Rayment *et al.*, 1993b; Schröder *et al.*, 1993). In good agreement with this view, functional studies have shown that the coupling efficiency between ATP hydrolysis and movement declines as the neck region is truncated or destabilized by removal of myosin light chains (Pollenz *et al.*, 1992; Itakura *et al.*, 1993; Lowey *et al.*, 1993; Uyeda and Spudich, 1993; VanBuren *et al.*, 1994; Waller *et al.*, 1995; Woodward *et al.*, 1995). Recently, Uyeda and co-workers produced myosins with neck regions of variable length by adding or truncating light chain binding motifs (Uyeda *et al.*, 1996). As predicted by the swinging neck–lever arm model, this study showed a linear relationship between the number of light chain binding sites and sliding velocity. Support for the lever arm hypothesis was also obtained by cryo-electron microscopy. Three-dimensional maps of myosin-decorated F-actin, obtained in the presence and absence of ADP, show little difference in the region of the globular motor domain; but there is reorientation of the LCBD, compatible with a step of at least 3.5 nm (Jontes *et al.*, 1995; Whittaker *et al.*, 1995). While these studies clearly indicate that the neck region acts as a lever, it remains controversial as to whether changes to the LCBD affect the interaction of the myosin motor with actin, binding of nucleotide, hydrolysis of ATP and communication between the actin and nucleotide binding sites.

In order to get more direct insight into the functional role of the LCBD, we engineered myosin head fragments (MHFs) consisting of the globular catalytic domain of *Dictyostelium discoideum* myosin fused to a structural motif whose dimensions and rigidity are similar to the LCBD. The best site for fusing an artificial lever arm to the catalytic domain was determined by generating a variety of motor domain constructs and screening their functional behavior using pre-steady-state kinetics. The shortest construct which behaved similarly to an S1-like construct was truncated at Arg761 of the *D.discoideum* myosin sequence (Geeves *et al.*, 1996). The equivalent residue in adult chicken skeletal muscle myosin is Lys782 (see Figure 1A). *Dictyostelium discoideum* α-actinin repeats were used as artificial lever arms. Each α-actinin repeat (Figure 1C) consists of ~120 residues and is predicted to form a left-handed coiled-coil consisting of three α-helices, thus creating very compact and rigid structural modules of ~6 nm length (Parry *et al.*, 1992; Yan *et al.*, 1993). Expression vectors for the production of two myosin motors with artificial lever arms were

© Oxford University Press

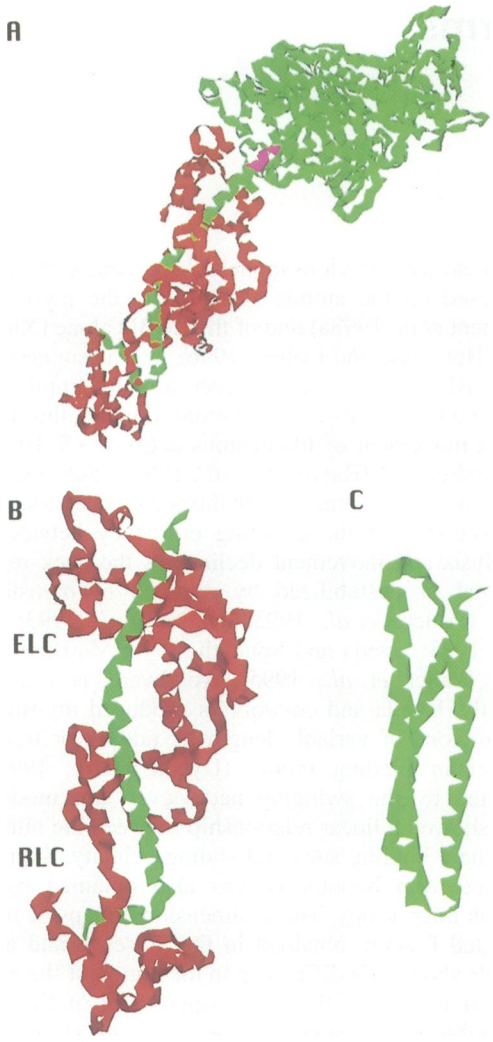

Fig. 1. Ribbon drawing of the chicken S1 structure (Rayment *et al.*, 1993b) and comparison of the scallop LCBD (Xie *et al.*, 1994) with the hypothetical structure of a single α-actinin repeat. (**A**) Ribbon diagram of S1 structure. The myosin heavy chain is shown in green with the exception of the region between residues 778 and 782. This region is shown in purple to indicate the position of Arg761, the last motor domain residue in M761-1R and M761-2R. Lys782, in the amino acid sequence of chicken skeletal S1, is the equivalent residue to Arg761 in the *D.discoideum* myosin heavy chain sequence. ELC and RLC are shown in red. (**B**) Ribbon diagram showing the overall fold of the scallop LCBD. The N-terminus of the myosin heavy chain fragment points to the top of the figure. The myosin heavy chain is shown in green, the ELC and RLC are shown in red. (**C**) Predicted fold of an α-actinin repeat (Parry *et al.*, 1992; Yan *et al.*, 1993). The figure was produced using the molecular graphics and analysis program Bioscape (Bioscape Inc.).

created. The resulting proteins, M761-1R and M761-2R, consist of the catalytic domain fused to one or two α-actinin repeats, respectively. The biochemical and functional competence of M761-1R and M761-2R was determined using pre-steady-state kinetics and *in vitro* motility assays.

This report addresses three questions raised by the lever arm hypothesis. Firstly, is it possible to replace the LCBD by a more simple structure of similar dimensions and rigidity and retain the motile properties? Secondly, does substitution of the LCBD alter the enzymatic properties of the myosin motor? Finally, do the motile properties

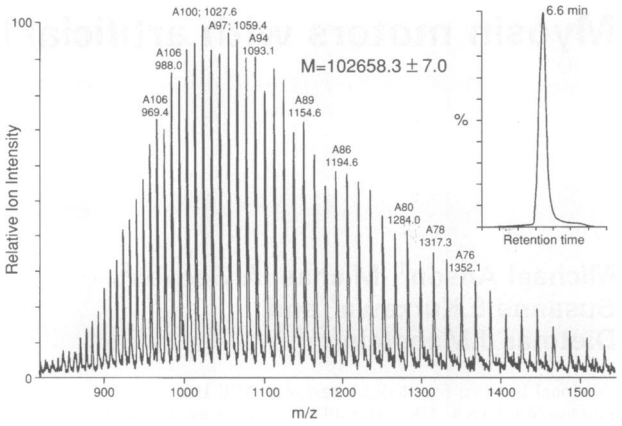

Fig. 2. Electrospray ionization mass spectrum of M761-1R produced in *D.discoideum*. Mass spectrometry was used to analyze the primary structure of the recombinant myosin motors and to identify any post-translational modifications. Perfusion reverse phase chromatography was performed to purify and desalt the protein. A 0.25 mm capillary perfusion column, filled with Poros R2 10 mm media, was used for on-line trapping before introduction of the protein to the mass spectrometry source. The insert in the upper right corner shows the elution profile monitored at 214 nm from this column.

change in the predicted way, if the length of the substituting domain differs from that of the LCBD?

Results

Expression and purification of recombinant myosin motors

M761-1R and M761-2R were produced with a C-terminal His tag to facilitate purification by Ni^{2+}-chelate affinity chromatography (Janknecht *et al.*, 1991; Manstein *et al.*, 1995). Typically, 2 mg of pure protein were obtained from 1 g of cells expressing either construct. The molecular mass of purified M761-1R and M761-2R was determined by electrospray mass spectrometry (ESMS) as 102 658 ± 7 (102 649.6) and 115 783 ± 14 (115 768.4), respectively. Values given in parentheses refer to the predicted molecular mass of the constructs (Figure 2). The S1-like construct M864 was purified as described previously (Manstein *et al.*, 1989).

Kinetic analysis of the myosin motors

The biochemical competence of M761-1R and M761-2R was determined using well established transient kinetics methods. The resulting data (Figure 3 and Table I) were interpreted in terms of the mechanism of rabbit skeletal muscle S1 and compared with similar measurements previously made for M864 (Ritchie *et al.*, 1993). In the absence of actin, we measured both the rate constant of ATP binding and the rate constant of ATP cleavage. The rate constants determined for M761-1R and M761-2R deviated by less than a factor of two from those determined for M864. Similarly, the affinity of ATP and ADP for acto·MHF changed by less than a factor of two, while the rate constants for ATP binding to acto·MHF and the maximum rate constant of ATP-induced dissociation of actin showed changes of <10%. Thus both the actin and nucleotide binding sites and the communication between the two sites show no significant changes between the

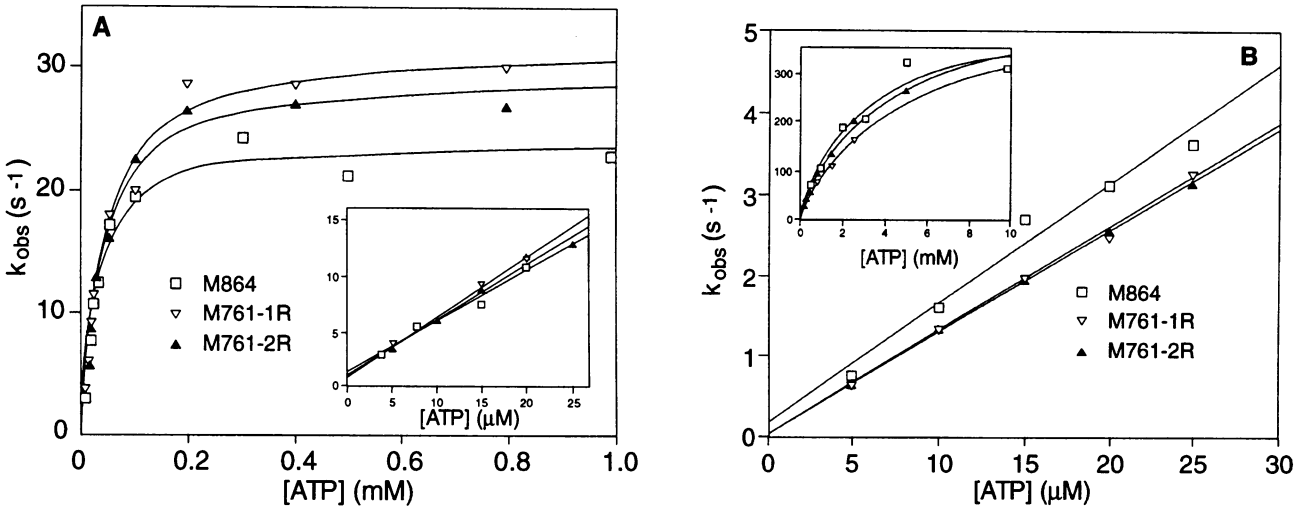

Fig. 3. Transient kinetic studies of MHFs and acto·MHFs. (**A**) The rate of ATP binding and hydrolysis by MHFs. MHF (0.5 μM) was mixed with an excess of ATP in a rapid mixing stopped-flow fluorimeter and the time-dependent changes in the intrinsic protein fluorescence recorded. The fluorescence increased and could be described by an exponential function $[(F_t-F_\infty) = (F_o-F_\infty)\exp(-k_{obs}\, n\, t)]$ and k_{obs} is plotted against [ATP]. The data set for each MHF was well described by a hyperbola, although the model for rabbit S1 does not predict a hyperbolic dependence of k_{obs} on [ATP]. The least squares fit to hyperbolae are shown superimposed, and k_{max}, the predicted k_{obs} at infinite [ATP] and $K_{0.5}$, the concentration of ATP when $k_{obs} = k_{max}/2$ were: M864 (□), k_{max} = 24/s, $K_{0.5}$ = 25.8 μM; M761-1R (▽), k_{max} = 29/s, $K_{0.5}$ = 34 μM; M761-2R (▲), k_{max} = 32/s, $K_{0.5}$ = 40 μM. The rate constant for the hydrolysis step ($k_{+3} + k_{-3}$) is defined from the value of k_{max}. The insert shows the same data at lower ATP concentrations and the lines are least squares best fits. The slope of the lines defines the apparent second order rate constant of ATP binding (K_1k_{+2}) and the values of the slopes are listed in Table I. (**B**) The rate of ATP-induced dissociation of acto·MHFs. Acto·MHF (0.25 μM) was mixed with an excess of ATP in the stopped-flow fluorimeter, and the increase in the fluorescence of a pyrene label, covalently attached to Cys374 of actin, recorded. The fluorescence increases when actin dissociates from the complex. The signal change was fitted to an exponential as in (A). At low ATP concentrations, k_{obs} was linearly dependent upon [ATP] and the best fit lines give slopes of: M864, 1.4×10^5/M/s; M761-1R , 1.2×10^5/M/s; M761-2R, 1.25×10^5/M/s. In each case, the intercept was not significantly different from zero. At higher ATP concentrations, the data could be fitted with hyperbolae as in (A). The fitted parameters are listed in Table I where $K_{0.5}$ defines $\boldsymbol{K_1}$ and k_{max} defines $\boldsymbol{k_{+2}}$.

S1-like M864 with native light chains and the two fusion constructs.

Direct functional characterization of the myosin motors

The similarities in the kinetic behavior of M761-1R and M761-2R to the S1-like fragment are also reflected in the *in vitro* motility data. When bound directly to a nitrocellulose-coated surface, M761-1R and M761-2R support actin moving at average rates of 107 and 169 nm/s, respectively (Figure 4A). This compares with a rate of 124 nm/s determined for M864 and of ~130 nm/s reported for two similar fragments (Manstein *et al.*, 1989; Itakura *et al.*, 1993). While the observed difference in the rates of actin movement over M761-1R and M761-2R correlates well with the prediction of the lever arm hypothesis, the significance of this result is compromised by the fact that full-length *D.discoideum* myosin moves at a 10- to 20-fold higher sliding speed (Uyeda and Spudich, 1993). The slower movement of single-headed fragments is generally explained by differences in the attachment of the motor to the surface. Accordingly, when the orientation of M761-1R and M761-2R was optimized using anti-histidine tag antibody mAb 13/45/3 (Zentgraf *et al.*, 1995) attached to the surface, velocities much closer to those observed with native *D.discoideum*, myosin were observed. Values of ~2.5 and ~3.3 μm/s were determined for M761-1R and M761-2R at 25°C, respectively (see Figure 4B). Under similar conditions but at 30°C, values of 1.9–3.1 μm/s were reported for native *D.discoideum* myosin (Ruppel *et al.*, 1994; Uyeda *et al.*, 1994).

Table I. Summary of rate constants

$$M + ATP \underset{k_{-1}}{\overset{k_{+1}}{\rightleftharpoons}} M.ATP \underset{k_{-2}}{\overset{k_{+2}}{\rightleftharpoons}} M^*.ATP \underset{k_{-3}}{\overset{k_{+3}}{\rightleftharpoons}} M.ADP.P_i$$

$$A.M + ATP \overset{\boldsymbol{K_1}}{\rightleftharpoons} A.M.ATP \overset{\boldsymbol{k_{+2}}}{\rightleftharpoons} A + M.ATP$$

$$A.M.ADP \overset{\boldsymbol{K_D}}{\rightleftharpoons} A.M + ADP$$

Rate constant	M864	M761-1R	M761-2R
$K_1\times k_{+2}$ ($M^{-1}s^{-1}$)	9.4×10^5	5.7×10^5	5.3×10^5
$k_{+3} + k_{-3}$ (s^{-1})	24	29	32
$\boldsymbol{K_1\times k_{+2}}$ ($M^{-1}s^{-1}$)	1.4×10^5	1.2×10^5	1.25×10^5
$\boldsymbol{K_1}$ (M^{-1})	330	286	170
$\boldsymbol{k_{+2}}$ (s^{-1})	450	447	650
$\boldsymbol{K_D}$ (μM)	94	140	190

The mechanism of nucleotide interaction with myosin and actomyosin derived from studies with muscle myosins is shown above the data. Rate and equilibrium constants in bold type refer to acto·MHF and normal type to the MHF in the absence of actin. The parameters are related to the constants obtained from the data in Figure 3 in the following way. From Figure 3A: the slopes of the fitted lines in the insert are equal to K_1k_{+2}; $k_{max} = k_{+3} + k_{-3}$. From Figure 3B: the slopes of the fitted lines are equal to $\boldsymbol{K_1k_{+2}}$; $k_{max} = \boldsymbol{k_{+2}}$; $K_{0.5} = 1/\boldsymbol{K_1}$. $\boldsymbol{K_D}$ was determined from the ADP inhibition of ATP-induced dissociation of acto·MHF as described previously (Ritchie *et al.*, 1993).

Discussion

In order to elucidate the complex molecular processes underlying the transduction of the chemical free energy

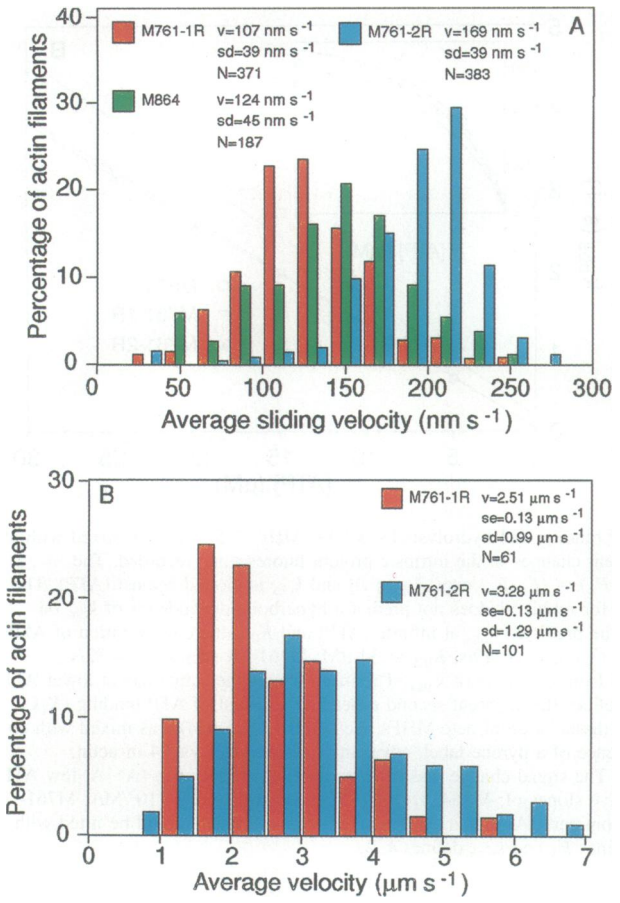

Fig. 4. Sliding velocity of F-actin filaments *in vitro* over recombinant MHFs. (**A**) Direct attachment of the MHFs to a nitrocellulose-coated bottom surface of a 50 μl flow cell. (**B**) In the case of M761-1R and M761-2R, the orientation for interaction with F-actin could be optimized by attachment via their C-terminal His tag to a surface that was previously decorated with mAb 13/45/31 (Zentgraf *et al.*, 1995). Histogram bars are shown for M864 (green), M761-1R (red) and M761-2R (blue). Abbreviations: v, velocity; sd, standard deviation; se, standard error; N, number of filaments.

of ATP hydrolysis into useful work by the actin–myosin motor system, it is necessary to use a variety of techniques. The combination of molecular biological methods for protein modification and engineering with the high resolution crystal structures of both actin and myosin enables systematic alterations in regions known or hypothesized to be important for motor function. Application of functional assays for biochemical and motile properties allows the structural modifications to be correlated with motor competence. Structural and functional studies ideally are carried out with a recombinant molecule that comes closest to the native protein. In the case of myosin, the proteolytic subfragment S1 is a very good and reliable model for studying myosin catalysis, kinetics, actin binding and motor function. However, S1-like fragments are notoriously difficult to produce in recombinant form and are hard to crystallize. As a consequence, structural and kinetics studies of recombinant myosin motors have been carried out mostly using the catalytic domain fragment alone. The problems associated with the use of S1-like fragments seem, to a large extent, to be caused by the three polypeptide chains that need to be co-expressed and properly assembled to make up such active motors.

A myosin motor complete with a lever arm consisting of just a single polypeptide chain should be much easier to produce and purify. Examination of the high resolution crystal structure of myosin S1 (Figure 1A) shows the LCBD as an independent domain with few contacts between the heavy chain and the ELC other than the IQ repeat target sequence. This makes it relatively straightforward to design C-terminal extensions of the catalytic domain that are predicted to function similarly to the LCBD. The choice of α-actinin repeats as a replacement for the LCBD was made for three reasons: firstly, the modular structure of the repeats facilitates the generation of motors with variable lever arm length; secondly, modeling of the repeat structure was aided by the extensive body of work on spectrin-like repeats; finally, the repeat sequences could be based on the *D.discoideum* α-actinin gene, thus avoiding any problems caused by the influence of codon usage on expression levels. *D.discoideum* exhibits a strong preference for AT-rich codons, and the influence of codon usage on the efficiency of protein production has been documented in at least one study (Dittrich *et al.*, 1994).

Modeling the catalytic domain fused to the rigid coiled-coil α-actinin repeat at the C-terminus in place of the LCBD showed that this construct would resemble the S1 structure but that the lever arm would be a little shorter, 6.5 nm compared with 8.5 nm. With two rigidly joined α-actinin repeats attached at the same residue, the predicted length of the lever arm became 13 nm; thus spanning the natural LCBD length between the two constructs. Both recombinant motor proteins could be produced at levels of ~12 mg/l in *D.discoideum* and rapidly purified to homogeneity by a selective enrichment step for functional myosin motors, followed by Ni^{2+}-chelate affinity chromatography (Manstein and Hunt, 1995). Examination by ESMS rather than just by SDS–PAGE confirmed, with resolution better than a single amino acid, that the desired monomeric constructs with the correct sequence and length were produced and purified (Figure 2). These data, together with the high expression levels, also suggest that both M761-1R and M761-2R fold to form the predicted stable structures.

Stopped-flow fast spectroscopy showed that the fusion of one or two α-actinin repeats to the M761 motor domain created molecular motors with kinetic properties nearly identical to those of the S1-like M864. Their actin and nucleotide binding properties and the communication between actin and nucleotide binding sites were little changed (Table I). Furthermore, while the catalytic domain alone shows very poor movement in *in vitro* motility assays, the attachment of α-actinin repeats as artificial lever arms produced functional motors that translate actin at velocities nearly proportional to the length of the attached lever (Figure 4). These results reveal that the observed changes in the actin motility assay result solely from alterations to the length of the lever arm rather than being an indirect effect on the kinetic properties of the catalytic domain.

A problem common to all actin-based *in vitro* motility assays, where the myosin is bound directly to a surface, is the unknown way in which the motor is attached. The point of attachment, its flexibility and the freedom of dynamic orientation may also affect translational velocity.

Further, molecules attached in an unfavorable orientation or not able to move freely may still interact with the actin polymers and reduce their velocity. This may explain the very low translational velocities seen for single-headed myosin constructs (<200 nm/s) compared with those with full-length wild-type *D.discoideum* double-headed myosin (2–3 μm/s) which approach those of fast double-headed skeletal myosins (4–8 μm/s). Thus the velocities which we observed with our constructs attached to nitrocellulose (Figure 4A) may reflect artifacts of the *in vitro* assay surface attachment. This conclusion is supported by our results using the C-terminal His tag to orient the motor construct by binding this tag to antibody molecules adhering to the surface. In this way, the motor molecules were attached at the extreme C-terminal end of the lever arm, raised above the nitrocellulose surface and given a large degree of orientational flexibility. As predicted, velocities then obtained were 20-fold higher and similar to those of full-length wild-type myosin (Figure 4B). Indeed, the velocities obtained (at 25°C) correlated with the estimated length of the lever arm from the atomic model : M761-1R, 6.5 nm and 2.5 μm/s , M761-2R, 13 nm and 3.3 μm/s.

Uyeda and co-workers (1996) used a different approach to varying the length of the lever arm. They either deleted one or both of the light chain binding sites or added a second binding site to the double-headed native *D.discoideum* myosin motor with full coiled-coil tail. In this way, they generated constructs with predicted lengths of 2, 6 and 13 nm from the putative fulcrum point of attachment of the LCBD to the start of the S2 region, and compared these with native wild-type myosin, to which they assigned a lever length of 8.5 nm. They used equilibrium ATPase measurements with or without 24 μM actin as indications of biochemical competence and the *in vitro* motility assay to quantify motor function. Binding the full-length myosin motor proteins, presumably via their long coiled-coil tails, directly to the surface, they found (at 30°C) actin velocities between 0.6 and 4 μm/s, directly proportional to the predicted lever arm length. These are close to the results presented here, and their velocity for wild-type myosin with LCBD length of 8.5 nm, 3 μm/s fits well with our data.

Both from inspection of the chicken S1 structure (Rayment *et al.*, 1993a) and from the functional properties observed for point mutations in the interface between the myosin heavy chain and ELC, that are associated with variants of human cardiac hypertrophy (Poetter *et al.*, 1996), one would expect a more critical role in mechano-chemical coupling for this region than observed with our constructs in the *in vitro* actin gliding assay. The most likely explanation for this discrepancy lies in the fact that this assay measures only one parameter of motor function. A motor has to produce force and movement, and the *in vitro* actin motility assay measures only the latter function against almost no load. The actin *in vitro* motility assay thus gives little indication as to how severely a certain mutation may affect the force production by the motor and about its functional competence *in vivo*.

We have shown that it is possible to replace the LCBD of *D.discoideum* myosin with rigid α-actinin constructs of variable length. The kinetics of such fusion proteins are closely similar to those of wild-type and they can be expressed and purified in large quantities. When orientated by binding to antibody, they have *in vitro* properties similar to those of the wild-type myosin, showing that they are fully functional motors, sustaining actin motility at velocities related to the lever arm length. Their high level of expression, ease of purification and functional competence should make such constructs extremely useful for further structural and functional studies of the myosin motor.

Materials and methods

Construction, expression and purification of recombinant myosin motors

The expression vectors used for the production of the myosin–α-actinin fusion constructs are based on pDXA-3H (Manstein *et al.*, 1995). The constructs were created by linking codon 761 of the *D.discoideum mhc*A gene (De Lozanne *et al.*, 1985) to codon 264 of the *D.discoideum* α-actinin gene (Noegel *et al.*, 1987). Constructs fused to one central repeat extended to codon 387 and constructs tagged with two repeats to codon 505 of the α-actinin gene. The peptide Leu–Gly–Ser separates the two sequences at the site of fusion, and both constructs are tagged at their C-terminus with the peptide Ala–Leu–$(His)_8$. All oligonucleotide linkers were optimized for *D.discoideum* codon bias. Modeling of the α-actinin repeat structure was performed using the programs PHD (Rost and Sander, 1993) and Bioscape (Bioscape Inc., Palo Alto, CA). DNA manipulations were done as described in Sambrook *et al.* (1989) and Egelhoff *et al.* (1991). M761-1R and M761-2R were overproduced in AX3-ORF^+ cells and purified by Ni^{2+}-chelate affinity chromatography as described previously (Manstein and Hunt, 1995; Manstein *et al.*, 1995). M864 was purified as described by Ritchie *et al.* (1993).

Electrospray mass spectrometry was performed on a Fisons VG Platform with on-line trapping as described by Aitken *et al.* (1995).

Stopped-flow experiments

All transient kinetic measurements were made using a Hi-Tech SF-61 stopped flow spectrofluorimeter. The details of this apparatus and its use for measuring the transient kinetics of rabbit S1 and *D.discoideum* MHFs have been described in our previous studies (Ritchie *et al.*, 1993; Woodward *et al.*, 1995). Actin was prepared from an acetone powder of rabbit skeletal muscle and labeled with pyrene iodoacetamide as described previously (Criddle *et al.*, 1985). Experimental conditions for all measurements were: 20°C, 0.1 M KCl, 5 mM $MgCl_2$, 20 mM HEPES adjusted to pH 7.0.

Motility assays

The *in vitro* assay was performed in a manner similar to that described previously (Anson, 1992) but with some modifications. Briefly, a 1.3NA 40× lens was used in epifluorescence with 546 nm excitation (Hg arc) and 580 nm emission band-pass (Omega filter set XF37). Filaments were imaged with a 4× lens on an intensified CCD TV camera (Darkstar 800) and recorded, via an image processor (Hamamatsu Argus 20) and time–date generator, by an S-VHS VCR (JVC BRS800-E). For slow moving filaments (Figure 4A), the TV format was converted from PAL to NTSC by a CVR22 digital converter (Snell and Wilcox). This permitted automated filament tracking using a VP110 digitizer at 1 frame/s utilizing Expert Vision software (Motion Analysis Inc.) running on a 486DX2-66 PC. For additional manual analysis of fast moving filaments (Figure 4B), tapes were replayed from the VCR to the Argus 20 and individual filaments tracked frame-by-frame using a mouse. Velocity was calculated from the positional change and the time code recorded on the tape. All solutions were kept on ice and the microscope stage was stabilized at 25°C.

Antibody-decorated surfaces were generated as follows: 75 μl of mAb 13/45/31 (Dianova GmbH, Hamburg), 200 μg/ml in phosphate-buffered saline, was infused into a 50 μl flow cell with a nitrocellulose-coated bottom surface. The cell was placed in a humidifier at 4°C for 60 min to allow the antibody to bind to the surface. It was flushed with 100 μl of bovine serum albumin (BSA), 10 mg/ml in 100 mM KCl and 50 mM HEPES pH 7.2, and incubated for 15 min at 25°C. This was repeated to ensure blocking of vacant protein binding sites on the surface. It was washed with 100 μl of 1 mg/ml BSA in 100 mM KCl and 30 mM HEPES pH 7.2. Then 50 μl of 1 mg/ml M761-1R or M761-2R in HAB (25 mM KCl, 25 mM HEPES pH 7.5, 4 mM $MgCl_2$ 1 mM EGTA, 5 mM dithiothreitol) was infused from each end of the flow-cell channel

and allowed to bind to the antibody-coated surface for 45 min in the humidifier at 4°C. After washing with 100 µl of 0.5 mg/ml BSA in HAB, 100 µl of 20 nM rabbit skeletal actin labeled with rhodamine–phalloidin was added and incubated for 2 min. The cell was washed again with 100 µl of 0.5 mg/ml BSA in HAB. Then 100 µl of AB (HAB with 100 µg/ml of glucose oxidase, 20 µg/ml of catalase, 5 mg/ml of glucose and 0.5 mg/ml of BSA, pH 7.5) was infused and the cell transferred to an inverted microscope (Zeiss Axiovert 35). After focusing and observation of the actin filaments in rigor, motion was initiated by infusing 100 µl of AB containing 2 mM ATP.

Acknowledgements

We would like to thank Dr C.Cohen for discussions and helpful suggestions, Dr A.A.Noegel for her gift of the *D.discoideum* α-actinin cDNA, Dr H.Faulstich for his gift of rhodamine–phalloidin, Dr J.A.Spudich for critical reading of the manuscript, Dr A.Aitken and S.Howell for the mass spectrometry, D.M.Hunt for expert technical assistance and N.Adamek for the preparation of pyrene-actin. The work was supported by the Medical Research Council (UK) and the Max Planck Society (Germany).

References

Aitken,A., Howell,S., Jones,D., Madrazo,J. and Patel,Y. (1995) 14-3-3 α and δ are the phosphorylated forms of Raf activating 14-3-3 β and ζ. *J. Biol. Chem.*, **270**, 5706–5709.

Anson,M. (1992) Temperature dependence and Arrhenius activation energy of F-actin velocity generated *in vitro* by skeletal myosin. *J. Mol. Biol.*, **224**, 1029–1038.

Cheney,R.E., Riley,M.A. and Mooseker,M.S. (1993) Phylogenetic analysis of the myosin superfamily. *Cell Motil. Cytoskeleton*, **24**, 215–223.

Criddle,A.H., Geeves,M.A. and Jeffrries,T. (1985) The use of actin labelled with N-(1-pyrenyl) iodoacetamide to study the interaction of actin with myosin subfragments and troponin/tropomyosin. *Biochem. J.*, **232**, 343–349.

De Lozanne,A., Lewis,M., Spudich,J.A. and Leinwand,L.A. (1985) Cloning and characterization of a nonmuscle myosin heavy chain cDNA. *Proc. Natl Acad. Sci. USA*, **82**, 6807–6810.

Dittrich,W., Williams,K.L. and Slade,M.B. (1994) Production of recombinant proteins in *Dictyostelium discoideum*. *Bio/technology*, **12**, 614–617.

Egelhoff,T.T., Titus,M.A., Manstein,D.J., Ruppel,K.M. and Spudich,J.A. (1991) Molecular genetic tools for study of the cytoskeleton in *Dictyostelium*. *Methods Enzymol.*, **196**, 319–334.

Geeves,M.A., Kurzawa,S., Hunt,D.M. and Manstein,D.J. (1996) Kinetic characterisation of different length fragments of the myosin head expressed in *Dictyostelium*. *Biophys. J.*, **70**, A267.

Goodson,H.V. and Spudich,J.A. (1993) Molecular evolution of the myosin family: relationships derived from comparisons of amino acid sequences. *Proc. Natl Acad. Sci. USA*, **90**, 659–663.

Houdusse,A. and Cohen,C. (1996) Structure of the regulatory domain of scallop myosin at 2 Å resolution: implication for regulation. *Structure*, **4**, 21–32.

Itakura,S., Yamakawa,H., Toyoshima,Y.Y., Ishijima,A., Kojima,T., Harada,Y., Yanagida,T., Wakabayashi,T. and Sutoph,K. (1993) Force-generating domain of myosin motor. *Biochem. Biophys. Res. Commun.*, **196**, 1504–1510.

Janknecht,R., De Martynoff,G., Lou,J., Hipskind,R.A., Nordheim,A. and Stunnenberg,H.G. (1991) Rapid and efficient purification of native histidine-tagged protein expressed by recombinant vaccinia virus. *Proc. Natl Acad. Sci. USA*, **88**, 8972–8976.

Jontes,J.D., Wilson Kubalek,E.M. and Milligan,R.A. (1995) A 32 degree tail swing in brush border myosin I on ADP release. *Nature*, **378**, 751–753.

Lowey,S., Waller,G.S. and Trybus,K.M. (1993) Skeletal muscle myosin light chains are essential for physiological speeds of shortening. *Nature*, **365**, 454–456.

Manstein,D.J. and Hunt,D.M. (1995) Overexpression of myosin motor domains in *Dictyostelium*: screening of transformants and purification of the affinity tagged protein. *J. Muscle Res. Cell Motil.*, **16**, 325–332.

Manstein,D.J., Ruppel,K.M. and Spudich,J.A. (1989) Expression and characterization of a functional myosin head fragment in *Dictyostelium discoideum*. *Science*, **246**, 656–658.

Manstein,D.J., Schuster,H.-P., Morandini,P. and Hunt,D.M. (1995) Cloning vectors for the production of proteins in *Dictyostelium discoideum*. *Gene*, **162**, 129–134.

Noegel,A., Witke,W. and Schleicher,M. (1987) Calcium-sensitive non-muscle alpha-actinin contains EF-hand structures and highly conserved regions. *FEBS Lett.*, **221**, 391–396.

Parry,D.A., Dixon,T.W. and Cohen,C. (1992) Analysis of the three-alpha-helix motif in the spectrin superfamily of proteins. *Biophys. J.*, **61**, 858–867.

Poetter,K. *et al.* (1996) Mutations in either the essential or regulatory light chains of myosin are associated with a rare myopathy in human heart and skeletal muscle. *Nature Genet.*, **13**, 63–69.

Pollenz,R.S., Chen,T.L.L., Trivinoslagos,L. and Chisholm,R.L. (1992) The *Dictyostelium* essential light chain is required for myosin function. *Cell*, **69**, 951–962.

Rayment,I., Holden,H.M., Whittaker,M., Yohn,C.B., Lorenz,M., Holmes, K.C. and Milligan,R.A. (1993a) Structure of the actin–myosin complex and its implications for muscle contraction. *Science*, **261**, 58–65.

Rayment,I., Rypniewski,W.R., Schmidtbase,K., Smith,R., Tomchick, D.R., Benning,M.M., Winkelmann,D.A., Wesenberg,G. and Holden, H.M. (1993b) Three-dimensional structure of myosin subfragment-1: a molecular motor. *Science*, **261**, 50–58.

Ritchie,M.D., Woodward,S.K.A., Manstein,D.J. and Geeves,M.A. (1993) Characterization of the interaction of a *Dictyostelium* myosin head fragment with actin and nucleotide. *Biophys. J.*, **64**, 359.

Rost,B. and Sander,C. (1993) Prediction of protein structure at better than 70% accuracy. *J. Mol. Biol.*, **232**, 584–599.

Ruppel,K.M., Uyeda,T.Q.P. and Spudich,J.A. (1994) Role of highly conserved lysine 130 of myosin motor domain: *in vivo* and *in vitro* characterization of site specifically mutated myosin. *J. Biol. Chem.*, **269**, 18773–18780.

Sambrook,J., Fritsch,E.F. and Maniatis,T. (1989) *Molecular Cloning: A Laboratory Manual*. Cold Spring Harbor Laboratory Press, Cold Spring Harbor, NY.

Schröder,R.R., Manstein,D.J., Jahn,W., Holden,H., Rayment,I., Holmes, K.C. and Spudich,J.A. (1993) Three-dimensional atomic model of F-actin decorated with *Dictyostelium* myosin S1. *Nature*, **364**, 171–174.

Uyeda,T.Q.P. and Spudich,J.A. (1993) A functional recombinant myosin II lacking a regulatory light chain-binding site. *Science*, **262**, 1867–1870.

Uyeda,T.Q.P., Ruppel,K.M. and Spudich,J.A. (1994) Enzymatic activities correlate with chimaeric substitutions at the actin-binding face of myosin. *Nature*, **368**, 567–569.

Uyeda,T.Q.P., Abramson,P.D. and Spudich,J.A. (1996) The neck region of the myosin motor domain acts as a lever arm to generate movement. *Proc. Natl Acad. Sci. USA*, **93**, 4459–4464.

VanBuren,P., Waller,G.S., Harris,D.E., Trybus,K.M., Warshaw,D.M. and Lowey,S. (1994) The essential light chain is required for full force production by skeletal muscle myosin. *Proc. Natl Acad. Sci. USA*, **91**, 12403–12407.

Vibert,P. and Cohen,C. (1988) Domains, motions and regulation in the myosin head. *J. Muscle Res. Cell Motil.*, **9**, 296–305.

Waller,G.S., Ouyang,G., Swafford,J., Vibert,P. and Lowey,S. (1995) A minimal motor domain from chicken skeletal muscle myosin. *J. Biol. Chem.*, **270**, 15348–15352.

Whittaker,M., Wilson Kubalek,E.M., Smith,J.E., Faust,L., Milligan,R.A. and Sweeney,H.L. (1995) A 35-Å movement of smooth muscle myosin on ADP release. *Nature*, **378**, 748–751.

Woodward,S.K.A., Geeves,M.A. and Manstein,D.J. (1995) Kinetic characterization of the catalytic domain of *Dictyostelium discoideum* myosin. *Biochemistry*, **34**, 16056–16064.

Xie,X., Harrison,D.H., Schlichting,I., Sweet,R.M., Kalabokis,V.N., Szent-Gyorgyi,A.G. and Cohen,C. (1994) Structure of the regulatory domain of scallop myosin at 2.8 Å resolution. *Nature*, **368**, 306–312.

Yan,Y., Winograd,E., Viel,A., Cronin,T., Harrison,S.C. and Branton,D. (1993) Crystal structure of the repetitive segments of spectrin. *Science*, **262**, 2027–2030.

Zentgraf,H., Frey,M., Schwinn,S., Tessmer,C., Willemann,B., Samstag,Y. and Velhagen,I. (1995) Detection of histidine-tagged fusion proteins by using a high-specific mouse monoclonal anti-histidine tag antibody. *Nucleic Acids Res.*, **23**, 3347–3348.

Received on June 4, 1996; revised on July 30, 1996